MADRID
inter.noise 2019
June 16 - 19
NOISE CONTROL FOR A BETTER ENVIRONMENT

Absorption and Transmission through Functionally-Graded Micro Perforated Panels

Bravo, Teresa[1]
Consejo Superior de Investigaciones Cientificas (CSIC)
Serrano 144, 28006 Madrid, Spain

Maury, Cédric[2]
Laboratory of Mechanics and Acoustics (CNRS LMA), Ecole Centrale Marseille
4 impasse Nikola Tesla, 13013 Marseille, France

de la Colina, Carlos[3]
Consejo Superior de Investigaciones Cientificas (CSIC)
Serrano 144, 28006 Madrid, Spain

ABSTRACT

To enhance absorption of noise without the introduction of active or massive components in the low frequency range, layouts of panels with micro-slits or micro-perforations have been considered as a non-fibrous alternative to conventional silencers and wall absorbents. These treatments are resonance absorbers composed of Micro-Perforated Panels (MPPs) with sub-millimetric apertures backed by air cavities with an absorption peak centred on the frequency of interest. For multilayer partitions, the parameters of each individual MPP can be tuned to broaden the global absorption performance. In this work we will further investigate the optimisation of multilayer MPP partitions considering not only the absorption but also the transmission performance of the control device. A theoretical model based on modal matching formulation and Fourier-Floquet expansion of the diffracted orders has been used for the optimisation of the graded structure constitutive parameters that maximises the acoustic dissipation of the system. It is found to be valid over a wider range of holes radii and separation distance with respect to effective impedance models, assuming MPPs with a constant holes pitch. A comparison against optimal impedance relationships from coherent perfect absorption criterion has also been carried out.

Keywords: Micro-perforated panels, low frequency noise control
I-INCE Classification of Subject Number: 35
http://i-ince.org/files/data/classification.pdf

1. INTRODUCTION

Current trend in noise control engineering is to design compact and

[1] teresa.bravo@csic.es
[2] cedric.maury@centrale-marseille.fr

lightweight panel structures able to lower the transmission of low frequency noise components, typically less than 500 Hz, while minimizing their reflection on one side or on both sides of the structure. In the aeronautical industry, this would help to design fuselage panels that could block during cruise conditions the external low-frequency jet noise components and the boundary layer noise that presents a peak at 600 Hz, but also to the improvement of the cabin acoustical comfort by reducing reflections on the panel internal side. This scenario also occurs at low speed flows in the automotive industry in order to reduce the boundary layer noise transmitted from the roof in a car cabin while achieving modal control of the interior noise, which is a challenging task without active systems at low frequencies. This problem obviously appears in building acoustics when designing an insulating wall, that should also be able to provide boundary absorption in the adjacent rooms, lowering their reverberation times and improving the speech intelligibility. In all cases, a strong constraint is to use compact and lightweight materials to reduce the embarked mass and fuel consumption in the transportation sector and the cost of the infrastructure in the building sector.

Of interest is to design acoustic metamaterials that can be engineered at subwavelength scales to control sound transmission and reflection on selective spectral bands, especially at low frequencies. The current study considers the use of multi-layer perforated panels in order to achieve these goals. However, we only consider normally incident plane waves unlike in the previous applications where the excitation can be from various incidences (jet noise) or modal (car cabin). It can even be spatially random including both acoustic and turbulent lengthscales (boundary layer noise). The normal incidence assumption is expected to provide a lower bound on the acoustical performance, but this is not clear cut. Also, in a first approach, we consider structures of infinite lateral extent that allow analytical tractability (especially the use of periodic Fourier series expansion of the pressure fields due periodic hole distribution), but the structures are in practice of finite extent with the effects of the lateral modes.

Previous works have focussed on sound transmission blockage by multi-layer perforates under normal or oblique incidence. The study of two perforates separated by a thin air gap, the so-called double fishnet, showed a transmission blockage at the frequency $f_b \approx c_0/(2.45\Lambda)$ for a wide range of panel thicknesses d_p and air gap widths d_g, with c_0 the air sound speed and Λ the holes spacing [1, 2]. This blockage is due to coupling between the odd-order modes of the open-ended pipes, constituted by two aligned holes, with the resonant side-branch due to the air gap at the pipe mid-point.

The side branch, when it is resonant, produces a maximum velocity (and zero pressure) at the pipe mid-point. It does not couple with the pipe even modes that also have zero pressure and maximum velocity at this point. But it strongly couples with the pipe odd modes that have a maximum pressure and zero velocity at this location [2]. This coupling creates a shift in frequency of these odd-order modes, therefore leaving a frequency bandwidth of zero transmission between the pipe modes resonant frequencies. However, because of millimetric hole spacing, this blockage frequency f_b occurs at high frequencies, that corresponds to 17 kHz in Bell *et al.* [2]. Moreover, although not quoted in the papers, simulations showed that in the zone of low transmission, large reflections occur on the perforate incident side, so at and around f_b, the system is insulating, but also highly reflecting. Hence, these pipe modes, also called Fabry-Perot modes, produce

maxima of transmission that also correspond to minima of reflection.

In order to broaden the frequency bandwidth of transmission blockage, a structure composed of multilayer periodically-spaced perforated panels has been studied [3] and its transmission properties verified experimentally under normal incidence. Sound transmission stop bands and pass bands were predicted by Bloch-Floquet analysis and observed up to 20 kHz when increasing the number of perforated panels. The stop bands result from the gap-holes resonant interaction described above and the pass band from a gathering of pipe modes that produce maxima of transmission. In Aközbeck model [3], a purely reactive effective impedance of each perforate was assumed so that the panels effective mass was only increased by the perforation ratio. The parametric studies showed that the broadest stop band occurred for equal panel and gap thicknesses and for panels with a low perforation ratio. Although not shown in the paper, it is accompanied by a frequency zone of large back-reflection toward the incident side. Also, the sound transmission at low frequencies in the first pass band is still significant.

In order to further reduce the low-frequency sound transmitted in the first pass-band, membrane-coated multi-layer perforates have been considered [4]. It was shown that the ultra thin membranes become very rigid at low frequencies so that they efficiently block the low-frequency sound transmitted on the first pass band, but this is made at the expense of large back reflections.

Recent studies have addressed the challenging problem of designing meta-materials of sub-wavelength thickness able to reduce both sound reflection and transmission, the so-called acoustic leakages. An idea is to design a structure that fully dissipates these leakages. A criterion, the critical coupling condition, has thus been formulated [5]. If the visco-thermal losses in the material exactly compensate the amount of leakages out of the system, then the incident power is fully dissipated within the system. In other words, the incident acoustical energy enters and is fully trapped and absorbed within the material, so that no energy comes out of the system, either from reflexion or transmission. This has been applied for rigidly-backed systems such as slits loaded by Helmholtz resonators [6] whose neck dissipative properties balance the amount of energy back-reflected. More recently, the critical coupling condition has been used to limit both reflection and transmission assuming a one-sided excitation of the system, e.g. to achieve a unidirectional perfect absorber. This has been applied to the design of a chirped multi-layer porous material [7] and of a rainbow trapping absorber made up of a series of Helmholtz resonators whose cavity depth monotonically increases in order to fulfil the critical coupling condition at each resonator position [8]. Note that these two latter configurations are special cases of axial functionally-graded materials, e.g. materials whose inner geometrical or mechanical properties gradually vary along the main propagation direction in order to achieve a given acoustical performance. Lately, a 3D printed functionally graded material (2.4 cm thick) has been designed constituted of three sections of increasing filling fraction (percentage of solid with respect to air in each section), the back section being a plain panel (100% filling fraction) to ensure near zero transmission. Impedance tube measurements showed that both reflection and transmission were near zero around 3 kHz [9].

The current study builds upon the idea of optimizing the absorption and transmission properties of a functionally-graded material made up of alternating layers of air and perforated plates whose filling fraction , $\varphi_f = d_p(1-\sigma)/(d_p + d_g)$ that depends on the perforation ratio σ, can be varied along the propagation

direction. However, a key direction is now to achieve a unidirectional perfect absorber at low frequencies, below 500 Hz, whilst keeping a subwavelength overall thickness of the system.

A theoretical model based on modal matching formulation is presented in Section 2.1 that predicts the pressure and velocity fields within the multilayer structure together with the normal incidence reflection and transmission coefficients that serve to the dissipation in the system. This model accounts for an arbitrary number of rigid perforated plates with a two-dimensional array of aligned holes, eventually submillimetric, separated by air gaps. Section 2.2 compares the predicted absorption and transmission performance against those obtained from impedance translation methods using two models of effective perforate impedances. Parametric studies are carried out in Section 3 to assess the dependency of the low transmission bands on the air gap and panel thicknesses as well as on the perforation ratio. This will lead to an assessment in Section 4 of the the effect of coating the last perforate transmitting face by an ultrathin membrane in order to enhance energy dissipation in a low frequency bandwidth. The main results and conclusions are summarized in Section 5.

2. MODAL MATCHING FORMULATION

In this section we will analyse the theory formulated by Bell *et al.* [2] based on the study of the acoustic double fishnets, as indicated in Fig. 1.

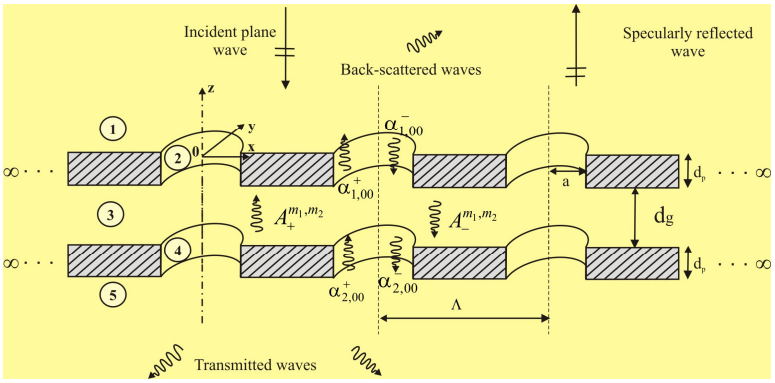

Figure 1. Cross-view of the double fishnet showing different regions for the modeling of the pressure field.

We will first outline the theoretical formulation of the model and continue with a comparison with other classical methods.

2.1 Model formulation

The theoretical analysis will take as the starting point a single fishnet, composed of a single infinite perforated plate. We analyze the problem by considering the different domains included in the configuration, starting by the first domain, situated above the perforated panel, where $z \geq 0$. Assuming the convention $e^{-i\omega t}$, we can express the pressure field in the first region as

$$p_1(x, y, z) = e^{-ik_0 z} + e^{ik_0 z} + \sum_{m_1=-\infty}^{\infty} \sum_{m_2=-\infty}^{\infty} R^{m_1,m_2} \Psi^{m_1,m_2}_{(x,y)} e^{-ik_z^{m_1,m_2} z}, \quad (1)$$

where $k_0 = \omega / c_0$ is the acoustic wavenumber, $\Psi_{(x,y)}^{m_1,m_2} = \exp\left[i\left(\frac{2m_1\pi}{\Lambda} \right) x \right] \exp\left[i\left(\frac{2m_2\pi}{\Lambda} \right) y \right]$, and the factors R^{m_1,m_2} are unknown quantities describing the complex field reflection coefficient for the pressure field. The integers pairs m_1, m_2 denote the orders of diffraction by the hole arrays of pitch Λ (separation distance between the holes or spatial period). The back-scattered waves are spatially periodic along x and y with period Λ.

The next domain includes the positions inside the holes, for $-d_p \le z \le 0$. When making the assumption that only plane waves propagate inside the holes ($f < 1.84 c_0 / 2\pi a$), we obtain a simplified expression for the pressure field in this region as

$$\mathrm{p}_2(r, z, \varphi) = \mathrm{p}_2(z) = \alpha_{00}^{+} e^{ik_0 z} + \alpha_{00}^{-} e^{-ik_0 z}, \tag{2}$$

where $\alpha_{00}^{\pm}$ correspond to the first order unknown coefficients for the in-going and out-going plane waves within the holes. Finally, we analyse the solution for the third domain, the transmission region, $z \le -d_p$, by expanding the transmitted pressure as

$$\mathrm{p}_3(x, y, z) = \sum_{m_1=-\infty}^{\infty} \sum_{m_2=-\infty}^{\infty} T^{m_1,m_2} \Psi_{(x,y)}^{m_1,m_2} e^{-ik_z^{m_1,m_2}\left(z + d_p\right)}, \tag{3}$$

where T^{m_1,m_2} are the unknown transmission coefficients. Eq. (3) is also a 2D spatial Fourier decomposition of the transmitted pressure that is periodic along x and y with period Λ.

When imposing appropriate boundary conditions for the continuity of the pressure and normal velocity at the panel-fluid domains interfaces using Eqs. (1) to (3), we obtain analytical expressions for the reflection and transmission coefficients. These descriptors will allow us to study the acoustic performance of the device.

2.2 Comparison against impedance translation methods

To validate the theoretical model, it is of interest to compare the dissipation, reflection and transmission results obtained from the modal matching formulation (MMF) described for alternate layers of air and perforates to those predicted by the impedance translation method that requires an effective impedance model of the perforates. A summary of this iterative method can be found in the reference [10].

Unlike the MMF that applied continuity of pressure and axial velocity at the entrance and exit of each panel hole cells, the impedance translation method considers each perforated panel as an effective element characterized by its effective transfer impedance Z_{MPP}. Z_{MPP} is the transfer impedance of one hole divided by the panel perforation ratio and can be described by Maa's [11] or Aközbeck's models [3].

The effective transfer impedance for a perforate with circular holes whose diameter and thickness are small compared to the acoustic wavelength is given by [10]:

$$Z_{MPP} = j\omega \frac{\rho_0 d_p}{\sigma} \left\{ \left[1 - \frac{2}{k\sqrt{-j}} \frac{J_1\left(k\sqrt{-j}\right)}{J_0\left(k\sqrt{-j}\right)} \right]^{-1} + \frac{16a}{3\pi d_p} \right\}, \tag{4}$$

with $\sigma = \pi a^2 / \Lambda^2$ the perforation ratio and $k = a / \sqrt{\eta / \rho_0 \omega}$ the perforate constant,

ratio of the holes radius a onto the viscous boundary layer thickness $\sqrt{\eta/\rho_0\omega}$. The first term in Eq. (4) accounts for viscous dissipation and inertial effects inside the holes, whereas the last term, $16a/(3\pi d_p)$, accounts for air motion inertia outside the holes. Eq. (4) can be identified to $Z_{eff} = j\omega\rho_{eff}d_p$, the low frequency effective transfer impedance across a fluid layer of thickness d_p and effective density ρ_{eff} provided that

$$\rho_{eff}^{Maa} = \frac{\rho_0}{\sigma}\left\{\left[1 - \frac{2}{k\sqrt{-j}}\frac{J_1\left(k\sqrt{-j}\right)}{J_0\left(k\sqrt{-j}\right)}\right]^{-1} + \frac{16a}{3\pi d_p}\right\}. \tag{5}$$

ρ_{eff}^{Maa} in Eq. (5) is complex, its real part describes the visco-thermic losses through the holes and its imaginary part the effective inertial effects. In particular, division by σ shows that $\rho_{eff}^{Maa} >> \rho_0$. Note that c_{eff}^{Maa} corresponds to c_0 under normal incidence.

Considering now the model presented by Aközbek *et al.* [3], where the transfer impedance takes the expression $Z_{MPP} = j\omega\rho_0 d_p/\sigma$, so that $\rho_{eff}^{Akoz} = \rho_0/\sigma$, a much simpler expression than Eq. (5), that does not describe visco-thermal dissipation, nor outside holes inertial effects. A comparison between the three models is presented in Fig. 2, where the modal matching method (left column), the Maa's model (centre column) and the Aközbek formulation (right column) has been used to calculate the dissipation, the reflected and transmitted powers as a function of the dimensionless frequency and dimensionless holes radii. The configuration selected is a three perforate system with holes spacing equal to $\Lambda = 8\,\text{mm}$, gap thickness $d_g = 8\,\text{mm}$ and perforate thickness $d_p = 8\,\text{mm}$. The frequency is varied between 10 Hz and 20 kHz whereas the holes radius was varied between 0.1 mm (MPP) and 3.9 mm (perforate), as seen on the y-axis of Fig. 2.

From the analysis of these figures, several conclusions can be made, starting with the model of Maa. The modal matching method compares well with Maa's impedance translation method at low frequencies, when $\Lambda/\lambda < 1/6 \approx 0.16$, and for small holes radii when $a < 0.3\Lambda$. This is an expected result since Maa's effective model is a priori valid for a sufficient number of holes per wavelength. Usually, the authors recommend at least 4 holes per wavelength but in this comparison, it is shown that 6 holes per wavelength are required ($\Lambda < \lambda/6$). At higher frequencies ($\Lambda/\lambda > 0.16$ or $f > 7\,\text{kHz}$), the model of Maa model is not predictive, unlike the MMF, as it only predicts the absorption peaks in the first band. It can be seen that these dissipation peaks correspond to transmission maxima and reflection minima: they are resonances due to air mass in the panel holes coupled to air stiffness in the gap. They increase when the holes radius increases. Indeed, the perforation ratio $\sigma = \pi a^2/\Lambda^2$ increases when a increases. From Eq. (5), the effective mass in the holes ρ_{eff}^{Maa} decreases (as $1/\sigma$) so that the hole-cavity resonance frequencies increase.

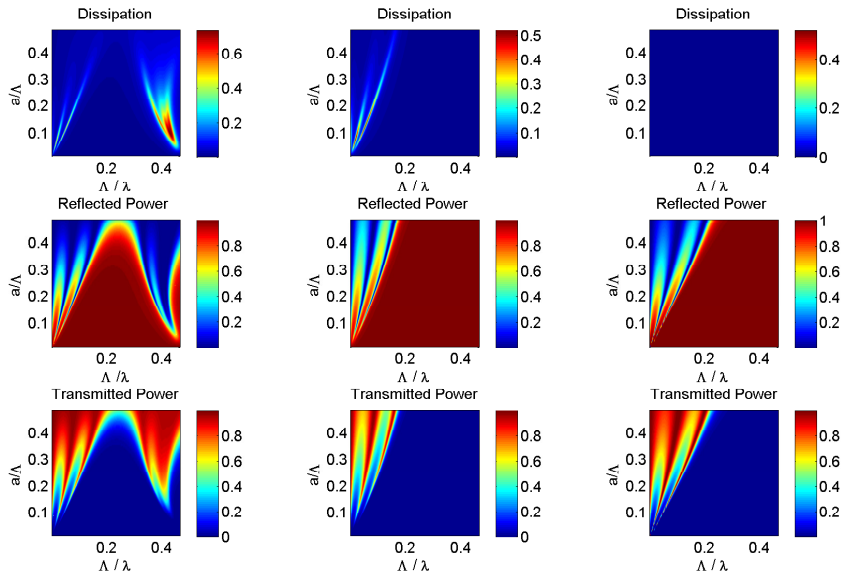

Figure 2. Dissipation, reflexion and transmitted power as a function of the dimensionless frequency and dimensionless radii holes when using the modal matching method (left column), the Maa's model (centre column) and the Aközbek formulation (right column)

Considering now the model of Aközbek for the impedance translation method shown in the last column, we could appreciate that like the model of Maa, it is only valid at low frequencies when $\Lambda < \lambda/6$ and the formulation for the simplified effective impedance, purely imaginary, is not able to predict the dissipation which is zero-valued everywhere. It can be clearly seen that this model is less accurate than Maa's model for very small holes radius where viscous effects in the holes play a role in the absorption, but it better predicts reflexion and transmission for perforates with a hole radius a greater than 0.3Λ, where inertia effects due to the air mass moving in the holes is dominant over viscous effects. It has to be outlined that at low frequencies, the holes radius plays an important role and should be less than 0.3Λ to maximize absorption. The use of larger holes may produce lower reflection, but higher transmission.

3. PARAMETRIC STUDIES

Parametric studies have been performed to evaluated the influence of three parameters (panel thickness d_p, gap thickness d_g and holes radius a) on the acoustic dissipation assuming a multi-layer partition constituted of six perforated panels with fixed holes spacing $\Lambda = 8\text{mm}$. The transmitted power is seen in Fig. 3 as a function of frequency and perforated panel thickness for given gap thickness and holes radius. It is noted that decreasing the holes radius decreases the perforation ratio σ given a fixed Λ. As appreciated in the first subplot, a pass-band zone appears independently of the panel thickness up to 32 kHz followed by a stop-band between 32 kHz and 38 kHz. Although only the transmission has been represented, similar conclusions could be drawn on the reflection and absorption coefficients. The purpose of the study consists of shifting the stop-band toward lower frequencies by a suitable selection of the constitutive parameters.

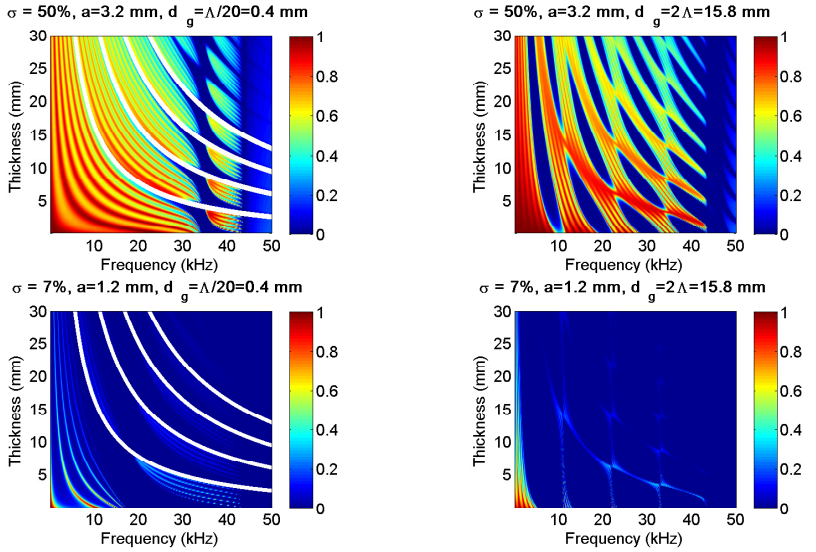

Figure 3. Transmitted power as a function of frequency and panel thickness for two different gap separations (left to right) and perforation ratios (top to bottom)

The first parameter that has been modified is the perforation ratio, starting from a large amount, $\sigma = 50\%$, associated to holes radius $a = 3.2\,\text{mm}$ (upper left subplot), and being decreased to $\sigma = 7\%$ associated to holes radius $a = 1.2\,\text{mm}$ (lower left subplot). As expected, decreasing the perforation ratio lowers the center frequency of the stop-band down to 20 kHz and increases its bandwidth. The same trend is observed in the right side of the figure, where the first stop band at 10 kHz is downshifted at 7 kHz and is much broader. Another parameter that affects the performance of the partition is the gap thickness, varied from a large value, $d_g = 2\Lambda = 15.8\,\text{mm}$, towards a smaller value $d_g = \Lambda/20 = 0.4\,\text{mm}$. It can be appreciated that it lowers the center frequency of the first stop band from 35 kHz down to 10 kHz, but this is achieved at the expense of an increase of the system total length $L = Q_p d_p + (Q_p - 1)d_g$.

We will then further investigate the physical configuration with moderate dimensions and a low perforation ratio that achieves the lowest transmission in the audible range (up to 20 kHz) including the corresponding reflection and transmission coefficients, as it can be seen in Fig. 4.

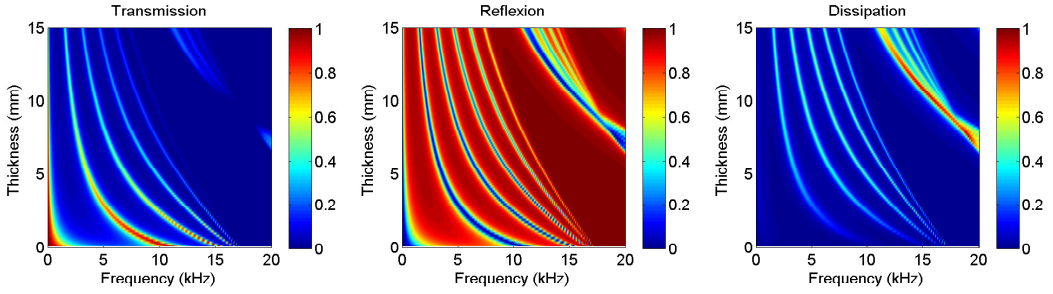

Figure 4. Transmission, reflection and dissipation coefficients for the partition composed of six perforated panels with $\sigma = 7\%$ and $d_g = 0.4\,\text{mm}$.

For the transmitted power we recognize a large blue zone around 17 kHz that corresponds to the first stop band with near-zero transmission. As explained in the introduction and in agreement with the work of Bell *et al.* [2], this stop-band occurs due to the odd-order modes resonance frequencies of the aligned holes, shifted away from the air gap side-branch resonances that are found at $f_b \approx c_0/(2.45\Lambda) \approx 17\text{kHz}$. It has very low transmission, but very high reflection due to a large impedance mismatch that occurs with the air on the incident side, which is against the goals of the control device, as we attempt to reduce both transmission and reflection, to achieve maximal dissipation in the partition. Having a closer look at the dissipation plot, we can appreciate locally a zone of high dissipation with both low reflection and transmission at 17 kHz for plate thicknesses above 7 mm. In this zone, the system fully dissipates the incident energy and nothing is transmitted, nor reflected. Unfortunately, this occurs at high frequencies and for thick panels. Below 17 kHz, red curves of high transmission and low reflection are observed. They are due to open holes acoustic resonances that decrease when increasing the panel thickness. There is some dissipation at these resonances, although they lead to undesirable high transmission for thin panels. Between these resonances, the transmission is low as desired, but the reflection is high and the dissipation is poor. This configuration corresponds to a large impedance mismatch of the system with the air as most of the incident wave is reflected.

As a general conclusion from the analysis of this configuration, we could state that the parameters analysed cannot fulfil the whole set of requirements and we should focus on a proper optimisation of the holes radius for each perforated panel. The goal is to shift these open holes acoustic resonances down to frequencies lower than 1kHz and to increase their modal overlap so that the dissipation would be maintained above a certain level between these resonances. This would lead to functionally-graded perforated panels (FGPP) with low leakages, e.g. low reflection and transmission, and high dissipation at low frequency.

4. EFFECT OF MEMBRANE COATING

This section will study the effect on the acoustic performance of the partition to add a thin membrane on the perforated panels, as illustrated in Fig. 5. The membrane parameters were taken to be the same as those used by Fan *et al.* [12] on a regular multi-layer perforate, fully-coated to block the sound transmission.

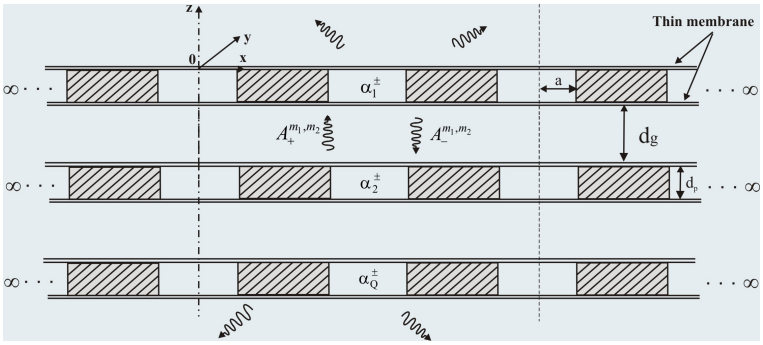

Figure 5. Thin membrane placed over the perforated panels to reduce the transmission performance.

The membrane is ultrathin (20 µm) and its resonance frequency (which was found to have a detrimental effect on the dissipation) is at high frequencies (well above 20 kHz). A model of the membrane transfer impedance, clamped along the circular edges of the holes was proposed by Bongard *et al*. [13]. In the present work, the MMF has been extended to account for the membrane resonances, but in the simulations, the membrane has only been included in the transmitting side of the partition as it was found to be sufficient to reduce the total transmitted power without enhancing back-reflections. Figure 6 shows the effect of coating by the thin membrane the transmitting face of a multi-layer FGPP, whose parameters have been optimized, on its dissipation, transmission and reflection coefficients below 200 Hz. It has to be clarified that for the optimized membrane-coated FGPP, the membrane is accounted for during the optimisation process, not added to the optimized FGPP without membrane.

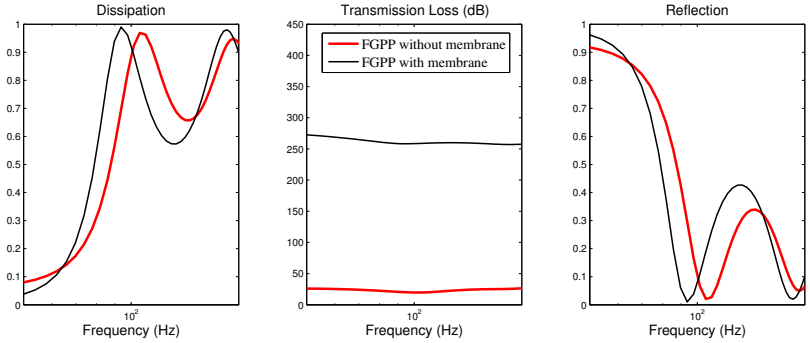

Figure 6. Dissipation (left), transmission loss (middle) and reflection coefficient (right) as a function of frequency for an optimised FGPP without membrane (red) and with a membrane on the transmitting panel (black).

From the analysis of this figure, several conclusions can be drawn. Adding a thin membrane on the last transmitting face completely blocks the sound transmitted due to the membrane that becomes very stiff at low frequencies. Note that without membrane, the sound transmitted by the optimized FGPP was already very low, so, despite high TL differences, the added value of the membrane on the transmission by the optimized FGPP is moderate. At low frequencies, the stiff membrane strongly back-reflects the wave that arrives in the last perforate. But this wave has already a low amplitude since it is strongly attenuated by the optimized holes radii, that have a chirped distribution. Therefore, membrane-coating does not further increase the absorption peak value. But it downshifts by 25% the peak resonance frequencies from 120 Hz down to 93 Hz due to the holes on the transmitting side closed by the membrane instead of being open holes.

For comparison purposes, the same physical configuration has been analysed for a regular FGPP with constant holes radius for all the MPPs. The corresponding results are presented in Fig. 7. As it can be seen, for the regular perforated material with holes radius $a = 0.6\,\text{mm}$, the situation changes substantially. Adding a thin membrane on the transmitting face blocks as before the sound transmitted at low frequencies, but then the added value of the membrane on sound transmission is important because the TL increases from 10 dB up to 170 dB. As before, the membrane strongly back-reflects the wave that arrives in the last perforate, but since this wave is moderately attenuated (the holes radii are not optimized), the MPP holes also attenuate the back-reflected wave, therefore increasing the dissipation peak from 0.4 to 0.9 and shifting its frequency down to 50 Hz.

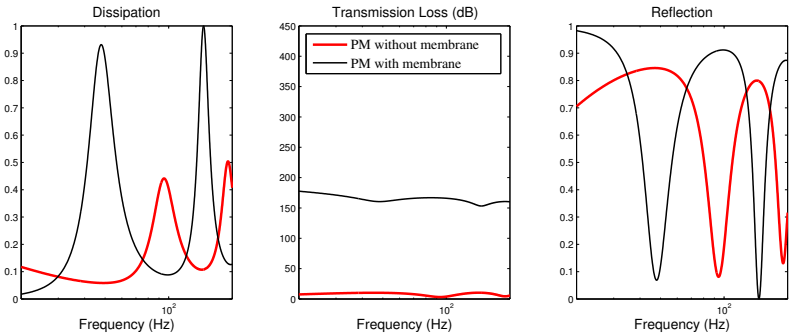

Figure 7. Dissipation (left), transmission loss (middle) and reflection coefficient (right) as a function of frequency for a regular FGPP (same holes radii) without membrane (red) and with a membrane at the transmitting panel (black).

In summary, membrane coating the transmitting face is more beneficial for a regular micro-perforated material than for an optimized FGPP. Although it has not been shown here, membrane-coating the front face of the material efficiently blocks the transmission but produces undesirable strong reflections, as observed by Fan *et al.* [12].

5. CONCLUSIONS

In this work, a modal matching method has been used to predict dissipation, transmission and reflection of a normal incident wave onto a multi-layer perforated partition with fixed hole spacing. Maa's impedance translation method has been compared against this analytical description and it has been found that it is only valid when there are at least 6 holes per wavelength, $f < c0/(6\Lambda)$, and the hole radius verifies $a < 0.3\ \Lambda$. The model presented is able to deal with an arbitrary number of perforated plates with holes not necessarily submillimetric. It has been extended to account for membrane-coated panels that account for an arbitrary axial distribution of holes radii as well as panel and gap thicknesses.

A set of parametric studies on regular perforates with the same holes radius has showed that increasing the gap thickness lowers the transmission stop band centre frequency, but at the expense of increasing the total length of the device. An alternative solution that has been verified is that decreasing the perforation ratio also downshifts the stop band and increases its width. This emphasizes the key role played by the holes radius.

Using the analytical modal matching method, the effect of an ultrathin membrane coating the transmitting side of the partition has been simulated and optimised on a FGPP. The optimised parameters bring moderate benefits on the dissipation (97% for L = λ/12). For comparison purposes, the same membrane-coated configuration has been used on the transmitting side of a regular multi-perforated panel. This configuration brings high benefits on the transmission blockage and on the first absorption peak, that reaches a value of 90% for L = λ/22.

Further works will include a more complete optimization of the FGPP to reduce the absorption dips between the peaks to get a uniform dissipation over a broader frequency range, as well as the experimental validation of the MMF in an impedance transmission tube from measurement of the scattering matrix in the plane wave domain. Finally, the authors would like to generalise the model to more complex excitations encountered in real-life for practical applications of the device, starting by considering oblique plane wave incidence.

6. ACKNOWLEDGEMENTS

This work has been funded by The Ministerio de Economía y Competitividad in Spain, project TRA2017-87978-R, AEI/FEDER, UE, "Programa Estatal de Investigación, Desarrollo e Innovación Orientada a los Retos de la Sociedad". It was supported in France by the Labex Mechanics and Complexity AAP2 managed by the Excellence Initiative Programme of Aix-Marseille University (A*MIDEX).

7. REFERENCES

1. J. Christensen, L. Martinez-Moreno and F.J. Garcia-Vidal, "*All-angle blockage of sound by an acoustic double-fishnet metamaterial*", Applied Physics Letters 97, 134106 (2010).
2. J. S. Bell, I. R. Summers, A. R. J. Murray, E. Hendry, J. R. Sambles, and A. P. Hibbins, "*Low acoustic transmittance through a holey structure*", Physical Review B 85, 214305 (2012).
3. N. Aközbek, N. Mattiucci, M. J. Bloemer M. Sanghadasa and G. D'Aguanno, "*Manipulating the extraordinary acoustic transmission through metamaterial-based acoustic band gap structures*", Applied Physics Letters 104, 161906 (2014).
4. L. Fan, Z. Chen, S.Y Zhang, J. Ding, X.J. Li and H. Zhang, "*An acoustic metamaterial composed of multi-layer membrane-coated perforated plates for low-frequency sound insulation*", Applied Physics Letters 106, 151908 (2015).
5. V. Romero-García, G. Theocharis, O. Richoux and V. Pagneux, "*Use of complex frequency plane to design broadband and sub-wavelength absorbers*", Journal of the Acoustical Society of America, 139 (6), 3395-3403, (2016).
6. N. Jiménez, H. Huang, V. Romero-García, V. Pagneux and J.P. Groby. "*Ultra-thin metamaterial for perfect and omnidirectional sound absorption*", arXiv:1606, 07776, 1-17, (2016).
7. N. Jiménez, V. Romero-García, A. Cebrecos, R. Picó, V.J. Sánchez Morcillos and L.M. García-Raffi. "*Broadband quasi perfect absorption using chirped multi-layer porous materials*", ArXiv 1610, 08011, 1-15, (2016).
8. N. Jiménez, V. Romero-García, V. Pagneux and J.P. Groby, "*Rainbow-trapping absorbers: Broadband, perfect and asymmetric sound absorption by subwavelength panels for transmission problems*", Scientic Reports, 7, 13595, (2017).
9. M. Guild, C. Rohde, M. Tothko and C. Sieck, "*3D printed acoustic metamaterial sound absorbers using functionally-graded sonic crystals*", Proceedings of Euronoise 2018, Crete, Athens, (2018).
10. T. Bravo, Cédric Maury and Cedric Pinhede, "*Enhancing sound absorption and transmission through flexible multi-layer micro-perforated structures*", J. Acoust. Soc. Am. 134 (5), 3363-3373, (2013).
11. D.-Y. Maa, "Potential of microperforated panel absorber," J. Acoust. Soc. Am. 104, 2861–2866 (1998).
12. L. Fan, Z. Chen, S.Y Zhang, J. Ding, X.J. Li and H. Zhang. "*An acoustic metamaterial composed of multi-layer membrane-coated perforated plates for low-frequency sound insulation*". Applied Physics Letters 106, 151908 (2015)
13. F. Bongard, H. Lissek, and J. R. Mosig, "*Acoustic transmission line metamaterial with negative/zero/positive refractive index*". Phys. Rev. B 82, 094306, (2010).